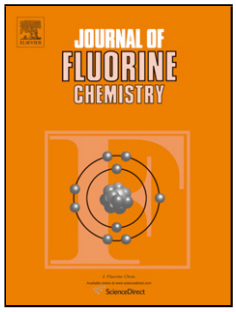

Title: Theoretical Studies on the Mechanism and Kinetics of the Hydrogen Abstraction Reactions from $C_4F_9OC_2H_5$ (HFE-7200) by OH and Cl radicals

Author: Abdorrasoul Hashemi Vahid Saheb S. Mohammad Ali Hosseini

PII: S0022-1139(16)30102-6
DOI: http://dx.doi.org/doi:10.1016/j.jfluchem.2016.04.014
Reference: FLUOR 8770

To appear in: *FLUOR*

Received date: 14-3-2016
Revised date: 26-4-2016
Accepted date: 28-4-2016

Please cite this article as: Abdorrasoul Hashemi, Vahid Saheb, S.Mohammad Ali Hosseini, Theoretical Studies on the Mechanism and Kinetics of the Hydrogen Abstraction Reactions from C4F9OC2H5 (HFE-7200) by OH and Cl radicals, Journal of Fluorine Chemistry http://dx.doi.org/10.1016/j.jfluchem.2016.04.014

Theoretical Studies on the Mechanism and Kinetics of the Hydrogen Abstraction Reactions from $C_4F_9OC_2H_5$ (HFE-7200) by OH and Cl radicals

Abdorrasoul Hashemi, Vahid Saheb* , S. Mohammad Ali Hosseini

Department of Chemistry, College of Science, Shahid Bahonar University of Kerman, Kerman, Iran

*Corresponding author. E-mail: [redacted]@mail.uk.ac.ir

Tel. & Fax: [redacted].

Graphical abstract

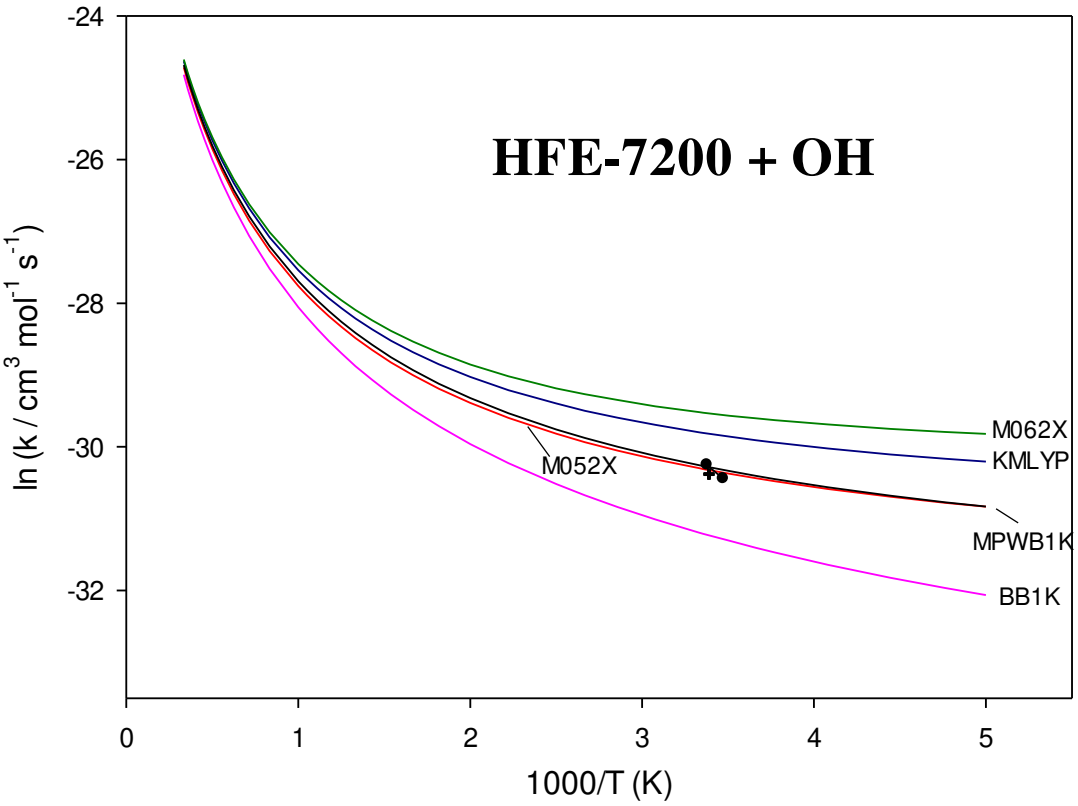

The thermal rate coefficients for the $C_4F_9OC_2H_5$ + OH reaction computed at different levels of theory.

Highlights

- The PES for the reaction $C_4F_9OC_2H_5$ + OH/Cl is explored.
- The rate coefficients are calculated by TST theory.
- The major reaction is the production of $C_4F_9OCH_5$ radical.
- The atmospheric lifetime of $C_4F_9OC_2H_5$ in computed theoretically.

Abstract

The potential energy surfaces for the hydrogen abstraction reactions from $C_4F_9OC_2H_5$ by OH (reaction R_A) and Cl (reaction R_B) radicals are investigated theoretically by density functional theory methods. The stationary points including reactants, saddle-points and products of the title reactions are optimized by using M06-2X density functional method along with the standard 6-31+G(d,p) basis set. The vibrational frequencies are computed at the same level of theory. More accurate energies are estimated by single-point calculations at the M05-2X/MG3S, M06-2X/MG3S, MPWB1K/MG3S, BB1K/MG3S and KMLYP/6-311++G(2d,2p) levels of theory. The computed barrier heights are slightly sensitive to the DFT method. Conventional transition state theory employing the tunneling for Eckart potential barrier is used to compute the thermal rate coefficients in the temperature range from 200 to 2000 K. The rate coefficients computed by using M05-2X/MG3S and MPWB1K/MG3S are in more agreement with the available experimental data. On the basis of the present computed rate coefficients, the atmospheric lifetime of the $C_4F_9OC_2H_5$ is estimated to be about 0.5 year.

Keywords: HFE-7200; hydroxyl radical; ab initio; transition state theory; atmospheric lifetime

Introduction

Ozone layer depletion and global warming have been two major environmental problems over the past four decades due to the emission of a diversity of halogen-containing compounds by different industries from earth surface and their accumulation in the atmosphere [1]. A worldwide effort have been made to replace the stable chlorofluorocarbons (CFC's) with the more reactive hydrogen-containing halocarbons such as hydrochlorofluorocarbons (HCFC's), hydrofluorocarbons (HCFC's) and hydrofluoroethers (HFE's). The latter halocarbons have shorter atmospheric lifetimes because they undergo hydrogen-abstraction reactions with reactive atmospheric species especially OH radicals, known as atmospheric detergents.

$C_4F_9OC_2H_5$ (HFE-7200) is a volatile liquid which is used in industry for the cleaning of electronic equipments, heat transfer agents in refrigeration systems and carrier fluids for lubricant deposition [2]. The atmospheric oxidation process of $C_4F_9OC_2H_5$ is initiated by it hydrogen-abstraction reaction with OH and Cl radicals. As a consequence, some groups have attempted to measure the rate coefficients for the reactions $C_4F_9OC_2H_5$ + OH (the reaction R_A) and $C_4F_9OC_2H_5$ + Cl (the reaction R_B). Wallington and coworkers [2] have measured the rate constant for the HFE-7200 + OH reaction by relative rate techniques and obtained value of 6.4×10^{-14} cm^3 $molecule^{-1}$ s^{-1} at 295 K. Bravo and collaborators [3] have employed a discharge flow technique coupled with mass-spectrometric detection to determine the Arrhenius parameters of the $C_4F_9OC_2H_5$+ OH reaction over the temperature range 288–368 K and reported the rate expression 6.9×10^{-11} cm^3 $molecule^{-1}$ s^{-1} exp(-2030/T). To the best of our knowledge, there are two experimental data for the reaction of Cl atoms with $C_4F_9OC_2H_5$. Wallington and coworkers [2] have reported the value of 2.7×10^{-12} cm^3 $molecule^{-1}$ s^{-1} at 295 K for $C_4F_9OC_2H_5$ + Cl reaction. Aranda and coworkers [4] have measured the rate constants for $C_4F_9OC_2H_5$ + Cl reaction by using a discharge flow mass spectrometric technique in the temperature range 234-333 K and obtained the rate expression as 3.7×10^{-11} cm^3 $molecule^{-1}$ s^{-1} exp(-852/T).

Due to its significance in atmospheric studies, we are inspired to do an ab initio study on the title reactions. Here, it is attempted to employ well-tested density functional theory (DFT) methods to investigate the potential energy surfaces (PES's) of the title reactions. Next, Conventional transition state theory (CTST) employing the tunneling for Eckart potential barrier is used to compute the thermal rate coefficients of the reactions R_A and R_B and to estimate the lifetime of $C_4F_9OC_2H_5$.

Computational details

Electronic-Structure Calculations: In the present work, the PES's for the reactions of OH and Cl radicals with $C_4F_9OC_2H_5$ are explored by M06-2X hybrid meta density functional theory (HMDFT) method [5] along with the standard 6-31+G(d,p) basis set and the structures for all of the stationary points, i.e., minimum energy structures and saddle points are optimized. The harmonic vibrational frequencies of the optimized geometries are calculated at same level of theory. Other HMDFT methods such as M05-2X [6],

MPWB1K [7] and BB1K [8] along with the larger MG3S basis [9] set are used to obtain more accurate energies. M05-2X, M06-2X, MPWB1K and BB1K methods have been developed by Truhlar and coworkers and optimized against various databases containing energetic data, bond lengths, vibrational frequencies and vibrational zero point energies and they are recommended for applications in kinetics and noncovalent interactions. The KMLYP method [10] developed by Kang and Musgrave is also employed to compute the molecular energies. In the latter DFT method, the exchange functional is obtained by mixing Slater exchange and exact exchange and the correlation functional is mix of Vosko, Wilk, Nusair (VWN) [11] and that of Lee, Yang, and Parr (LYP) [12] correlation functionals. The predicted reaction barrier heights by KMLYP method is proved to have the same accuracy as CBS-APNO, and transition state barriers and reaction enthalpies have smaller errors in comparison with B3LYP, BHandHLYP, and G2.All of the quantum chemical calculations are carried out by Gaussian 09 package of programs [13].

Rate Constant Calculations: Having the molecular parameter for the reactants and transition states, Conventional Transition State Theory (CTST) [14-20] is used to compute the thermal rate constants for the rations R_A and R_B in the temperature range between 250-2000 K. In the CTST, canonical rate constant is computed according to the following equation:

$$k(T) = \Gamma \frac{k_B T}{h} \frac{Q_t^{\ddagger} Q_r^{\ddagger}}{Q_t Q_r Q_v} \exp(-E_0 / k_B T) \qquad (1)$$

where h is Planck's constant, k_B is Boltzmann's constant, T is the temperature, Q_t, Q_r and Q_v are the translational, rotational and vibrational partition functions for the reactants, respectively; and the $Q_t^{\ddagger}$ and $Q_r^{\ddagger}$ represent corresponding values for transition state. Γ in the above equation is the ratio of quantum-mechanical barrier-crossing rate to classical-mechanical barrier-crossing rate (tunneling effect) which is computed for an Eckart potential barrier according to following equation [21-23]:

$$\Gamma = \exp(V_1 / RT) \int_0^{\infty} \kappa \exp\left(-E / k_B T\right) dE / k_B T \qquad (2)$$

where V_1 is the height of the potential barrier towards the exothermic direction of the reaction, and κ is the transmission probability for tunneling given by

$$\kappa(T) = 1 - \frac{\cosh 2\pi(a-b) + \cosh 2\pi d}{\cosh 2\pi(a+b) + \cosh 2\pi d} \qquad (3)$$

The parameters in above equation are given by the following equations

$$a = \frac{[\alpha_1 \xi]^{1/2}}{\pi}\left(\frac{1}{\alpha_1^{1/2}} + \frac{1}{\alpha_2^{1/2}}\right)^{-1} \quad (4)$$

$$b = \frac{[\alpha_1(1+\xi) - \alpha_2]^{1/2}}{\pi}\left(\frac{1}{\alpha_1^{1/2}} + \frac{1}{\alpha_2^{1/2}}\right)^{-1} \quad (5)$$

$$d = \frac{1}{\pi}[\alpha_1 \alpha_2 - 2\pi^2/16]^{1/2} \quad (6)$$

$$\alpha_1 = 2\pi V_1/h\nu^* \quad (7)$$

$$\alpha_2 = 2\pi V_2/h\nu^* \quad (8)$$

$$\xi = E/V_1 \quad (9)$$

where ν^* in imaginary frequency of the saddle-point, V1 and V2 are the heights of the potential barrier towards the exothermic direction and its reverse reaction, respectively. In this research work, MULTIWELL program package [24] is used to compute the thermal rate coefficients.

Results and discussion

On the basis of the present theoretical study, the following reaction paths can be considered for the hydrogen abstraction reactions from $C_4F_9OC_2H_5$ by OH and Cl radicals:

$C_4F_9OCH_2CH_3 + OH \rightarrow C_4F_9OCH_2CH_2 + H_2O$ R_{A1}

$C_4F_9OCH_2CH_3 + OH \rightarrow C_4F_9OCHCH_3 + H_2O$ R_{A2}

$C_4F_9OCH_2CH_3 + Cl \rightarrow C_4F_9OCH_2CH_2 + HCl$ R_{B1}

$C_4F_9OCH_2CH_3 + Cl \rightarrow C_4F_9OCHCH_3 + HCl$ R_{B2}

According to the computed energies at the MPWB1K/MG3S level of theory, the mechanism of the hydrogen-abstraction reactions from $C_4F_9OC_2H_5$ by OH radical can be described as follows. The reaction proceed through a van der Waals complex, denoted as vdWiA, with an energy of 12.85 kJ mol^{-1} lower that the reactants. This complex is formed via hydrogen bonding between H atom of OH radical and O atom of $C_4F_9OC_2H_5$. Next, hydrogen atoms transfer from $C_4F_9OC_2H_5$ to OH radicals through the transition state structures TS1A and TS2A leading to van der Waals complexes vdWf1A and vdWf2A, respectively. The energies of the transition states TS1A and TS2A relative to reactants

are 12.43 and 4.10 kJ mol^{-1}, respectively. In the van der Waals complexes vdWf1A and vdWf2A, water molecules are attached to the produced radicals via hydrogen bonding interactions. The relative energies of the complexes vdWf1A and vdWf2A are -70.41 and -88.24 kJ mol^{-1} and dissociate to give the products $C_4F_9OCH_2CH_2$ + H_2O (P1A) and $C_4F_9OCHCH_3$ + H_2O (P2A), respectively. The products P1A and P2A are -55.85 and -78.24 kJ mol^{-1} more stable than the reactants, respectively. The structure of the reactants and transition states of the $C_4F_9OC_2H_5$ + OH reaction are depicted in Figure 1. The z-matrices of the reactants, van der Waals complexes and transition states are provided in the Supplemental Information. It is noteworthy to mention that the most stable conformations of the HFE-7200 and transition states are used in the rate constant calculations. It is found that the transition state structures used in the present calculations are relatively more stable than their other conformations. We think that this is due to the hydrogen bonds between H atom of OH radicals, and O or F atoms of HFE-7200. Nonetheless, most sophisticated approaches are needed to investigate these hydrogen bonds.

The reaction $C_4F_9OC_2H_5$ + Cl proceed through a similar mechanism. It occurs via formation of a van der Waals complex, denoted as vdWiB, with an energy of 6.24 kJ mol^{-1} lower that the reactants. Next, hydrogen atoms transfer from $C_4F_9OC_2H_5$ to Cl atoms through the transition state structures TS1B and TS2B leading to van der Waals complexes vdWf1B and vdWf2B, respectively. The energies of the saddle-point structures TS1A and TS2A relative to reactants are +8.93 and -3.64 kJ mol^{-1}, respectively. The relative energies of the complexes vdW1fB and vdW2fB are –15.3 and -35.51 kJ mol^{-1} and dissociate to give the products $C_4F_9OCH_2CH_2$ + HCl (P1B) and $C_4F_9OCHCH_3$ + HCl (P2B), respectively. The products P1B and P2B are -5.13 and -27.52 kJ mol^{-1} more stable than the reactants ($C_4F_9OC_2H_5$ + Cl), respectively.

The computed energies at different levels of theory are given in Table1. As can be seen, there is a good consistency between energies obtained for stationary points of these reactions at various levels of theory. The potential energy profile of the reactions A and B are depicted in Figures 2 and 3. Nevertheless, the barrier heights calculated by BB1K/MG3S method are slightly overestimated and those by M06-2X/MG3S are underestimated. The principal moments of inertia harmonic and the vibrational

frequencies of the reactants and transition states, calculated at the M06-2X/6-31+G(d,p) level of theory, are provided in Table 2S in the Supplemental Information.

The low vibrational frequencies in the $C_4F_9OCHCH_3$ and transition states (underlined in Table 1S in the Supplemental Information) corresponds to hindered internal rotations along C-C and C-O bonds. It is attempted to compute the sum of states for these degrees of freedom, by employing the ro-vibrational G matrix-based algorithm of Harthcock et al. [25] for the effective reduced masses for one-dimensional torsions. However, it is found that the low-vibrational frequencies correspond to very similar motions in the $C_4F_9OCHCH_3$ and the transition states of the reactions R_{A1}, R_{A2}, R_{B1} and R_{B2} and their corresponding partition functions are canceled from the numerator and denominator of the equation (1).

Having the molecular parameters such as the vibrational frequencies and the principal moments of inertia harmonic of the reactants and transition states, and barrier-height energies, CTST is employed to calculate the thermal rate coefficients for all reaction paths over the temperature range of 200 to 2000 K. The computed overall rate coefficients for the hydrogen-abstraction reaction from $C_4F_9OC_2H_5$ by OH radicals employing different computed barrier heights are shown in Figure 4. To the best of our knowledge, two experimental study is reported on the kinetics of the hydrogen-abstraction from $C_4F_9OC_2H_5$ by OH radical [2,3]. These data are given in Figure 4 for the purpose of comparison. As can be seen from Figure 4, the computed rate coefficients by using MPWB1K and M05-2X barrier heights are in accordance with the available experimental data. The computed rate coefficients employing M06-2X and KMLYP barrier-heights are slightly overestimated and those employing BB1K saddle-point energies are underestimated.

In the present work, it is attempted to choose well-tested DFT methods for kinetics calculations. Nevertheless, each DFT method has its pros and cons and, in addition, the molecular system studied in the present work is large. So the average of the computed barrier heights by different methods are also employed to compute the rate coefficients (the dark solid line in Figure 4). As can be seen from Figure 4, the computed rate coefficients by using the average of the computed barrier heights are in accordance with the available experimental data. It is revealed from the present kinetics calculations that

the dominant reaction channel is the product channel $C_4F_9OCHCH_3$ + OH (P_{A2}). The computed rate coefficients for two hydrogen-abstraction reaction paths from $C_4F_9OCH_2CH_3$ by OH radicals are shown in Figure 1S in the Supplemental Information. The branching ratio for the reaction channel R_{A2} varies from 0.969 at 200 K to 0.830 at 1000 K.

The computed overall rate coefficients for the reaction of $C_4F_9OC_2H_5$ with Cl atom by using different saddle-point energies are shown in Figure 5. To date, two experimental studies [2,4] are reported on the kinetics of the hydrogen-abstraction from $C_4F_9OC_2H_5$ by Cl atom which are plotted in Figure 5 for the purpose of comparison. Figure 2 reveals that consistent rate coefficients are obtained when different barrier heights are used and the computed rate coefficients are in accordance with the available experimental data. However, the computed rate coefficients employing BB1K barrier-heights is slightly underestimated. The computed rate coefficients for two hydrogen-abstraction reaction paths from $C_4F_9OC_2H_5$ by Cl atoms are depicted in Figure 2S in the Supplemental Information. The branching ratio for the reaction channel R_{B2} varies from 0.974 at 200 K to 0.526 at 1000 K. The dominant reaction channel is found to be the product channel $C_4F_9OCHCH_3$ + Cl (P_{B2}).

Regarding the atmospheric implications, the lifetime of the $C_4F_9OC_2H_5$ could be estimated via the rate constant of the $C_4F_9OC_2H_5$ + OH reaction at 272 K. The rate constant at 272 K and tropospheric lifetime of CH_3CCl_3 are considered as benchmark quantities for estimating the lifetimes for other atmospherically important species [26]. As a consequence, the lifetime of the $C_4F_9OC_2H_5$ could be obtained by the following equation:

$$\tau_{C4F9OC2H5} = \frac{k_{CH3CCl3}}{k_{C4F9OC2H5}} \tau_{CH3CCl3}$$

$k_{CH3CCl3}$ and $k_{C4F9OC2H5}$ are the rate coefficients for the reactions of CH_3CCl_3 and $C_4F_9OC_2H_5$ with OH radicals at 272 K, respectively. $\tau_{CH3CCl3}$ and $\tau_{C4F9OC2H5}$ are the tropospheric lifetimes of CH_3CCl_3 and $C_4F_9OC_2H_5$, respectively. The literature values for $k_{CH3CCl3}$ at 272 K and $\tau_{CH3CCl3}$ are 6.0×10^{-15} cm^3 molecule^{-1} s^{-1} [27] and 5.99 years [28], respectively. According to the present calculations, the lifetime of $C_4F_9OC_2H_5$ is estimated to be about 0.5 years when an average of computed barrier heights by different DFT methods are employed. The present predicted value for the atmospheric lifetime of

$C_4F_9OC_2H_5$ is lower than the value of 0.9 estimated by Bravo et al. [3]. Bravo and coworkers have estimated the rate coefficient for $C_4F_9OC_2H_5$ + OH at 272 K on the basis of their Arrhenius expression obtained for the temperature range 288-368 K. Their measured activation energy is slightly higher the value predicted in this theoretical work leading higher value for atmospheric lifetime of $C_4F_9OC_2H_5$. It is noteworthy to mention that 0.37 kcal mol^{-1} error in estimating activation energy leads to an error in estimating lifetimes by a factor of 2. Therefore, estimating correct barrier heights play crucial role in evaluating the lifetimes of atmospherically important compounds. The present theoretical study may inspire further experimental researches on the kinetics and tropospheric lifetime of $C_4F_9OC_2H_5$.

Finally, on the basis of the computed rate coefficients having the best consistency with the available experimental data, it is attempted to present the following four-parameter rate expression [29] for the temperature dependence of title reactions.

$$k(T) = A(T/K)^n \exp\left[\frac{-E(T+T_0)}{T^2+T_0^2}\right] \qquad (11)$$

The computed rate constants for the reactions R_A to R_B are fitted to the equation 11. The parameters *A, n, E* and T_0 for the reaction R1 are 1.06×10^{-13} cm^3 mol^{-1} s^{-1}, 0.6116, 1589 K and 467 K, respectively. The corresponding values for the reaction R2 are 9.34×10^{-14} cm^3 mol^{-1} s^{-1}, 1.02, 1265 K and 500 K, respectively.

Conclusion

In this research, the rate coefficients of the hydrogen abstraction reactions from $C_4F_9OC_2H_5$ by OH and Cl radicals are investigated theoretically. The energies and other molecular properties of the stationary points on the potential energy surfaces the title reactions are computed by using DFT methods. The geometry optimizations and the calculation of vibrational frequencies are performed at the M06-2X/6-31+G(d,p) level of theory. Better estimations of the barrier heights of the reactions are obtained by single-point energy calculations by M05-2X, M06-2X, KMLYP, MPWB1K and BB1K methods along with the larger MG3S basis sets. The calculated rate coefficients are slightly sensitive to the computed barrier heights. The calculated rate constants are in good agreement with the available experimental data when the barrier heights computed at the

M05-2X and MPWB1K levels are employed. On the basis of the present calculations, the lifetime of the $C_4F_9OC_2H_5$ is estimated to be about 0.5 year.

Acknowledgements

The authors thanks Professor John R. Barker for providing the MultiWell-2014.1 programs. The financial support of Shahid Bahonar University of Kerman Research Council for this research is gratefully acknowledged.

References

[1] UNEP/WMO, Scientific Assessment of Ozone Depletion: 2014; World Meteorological Organization Global Ozone Research and Monitoring Project—Report No. 55.

[2] L.K. Christensen, J. Sehested, O.J. Nielsen, M. Bilde, T.J. Wallington, A. Guschin, L.T. Molina, M.J. Molina, J. Phys. Chem. A 102 (1998) 4839-4845.

[3] I. Bravo, Y. Díaz-de-Mera, A. Aranda, K. Smith, K.P. Shine, G. Marston, Phys. Chem. Chem. Phys. 12 (2010) 5115–5125.

[4] A. Aranda, Y. Díaz-de-Mera, I. Bravo, D. Rodríguez, A. Rodríguez, E. Martínez, Environ. Sci. Technol. 40 (2006) 5971-5976.

[5] Y. Zhao, D.G. Truhlar, Theory Chem. Acc. 120 (2008) 215-241.

[6] Y. Zhao, N.E. Schultz, D.G. Truhlar, J. Chem. Phys. 123 (2005) 161103,1-4.

[7] Y. Zhao, D.G. Truhlar, J. Phys. Chem. A 108 (2004) 6908-6918.

[8] Y. Zhao, B.J. Lynch, D.G. Truhlar, J. Phys. Chem. A 108 (2004) 2715-2719.

[9] B.J. Lynch, Y. Zhao, D.G. Truhlar, J. Phys. Chem. A 107 (2003) 1384-1388.

[10] J.K. Kang, C.B. Musgrave, J. Chem. Phys. 115 (2001) 11040-11051.

[11] S.H. Vosko, L. Wilk, M. Nusair, Can. J. Phys. 58 (1980) 1200-1211.

[12] C. Lee, W. Yang, R.G. Parr, Phys. Rev. B 37 (1988) 785-789.

[13] M.J. Frisch, G.W. Trucks, H.B. Schlegel, G.E. Scuseria, M.A. Robb, J.R. Cheeseman, G. Scalmani, V. Barone, B. Mennucci, G.A. Petersson, H. Nakatsuji, M. Caricato, X. Li, H.P. Hratchian, A.F. Izmaylov, J. Bloino, G. Zheng, J.L. Sonnenberg, M. Hada, M. Ehara, K. Toyota, R. Fukuda, J. Hasegawa, M. Ishida, T. Nakajima, Y. Honda,

O. Kitao, H. Nakai, T. Vreven, J.A. Montgomery, Jr., J.E. Peralta, F. Ogliaro, M. Bearpark, J.J. Heyd, E. Brothers, K.N. Kudin, V.N. Staroverov, R. Kobayashi, J. Normand, K. Raghavachari, A. Rendell, J.C. Burant, S.S. Iyengar, J. Tomasi, M. Cossi, N. Rega, J.M. Millam, M. Klene, J.E. Knox, J.B. Cross, V. Bakken, C. Adamo, J. Jaramillo, R. Gomperts, R.E. Stratmann, O. Yazyev, A.J. Austin, R. Cammi, C. Pomelli, J.W. Ochterski, R.L. Martin, K. Morokuma, V.G. Zakrzewski, G.A. Voth, P. Salvador, J.J. Dannenberg, S. Dapprich, A.D. Daniels, O. Farkas, J.B. Foresman, J.V. Ortiz, J. Cioslowski, D.J. Fox, Gaussian 09, Revision A.1, Gaussian, Inc., Wallingford, CT, 2009.

[14] A. Tweedale, K.J. Laidler, J. Chem. Phys. 53 (1970) 2045-2052.

[15] M.A. Eliason, J.O. Hirschfelder, J. Chem. Phys. 30 (1959) 1426-1434.

[16] B.C. Garrett, D.G. Truhlar, J. Phys. Chem. 83 (1979) 1052-1079.

[17] B.C. Garrett, D.G. Truhlar, J. Phys. Chem. 83 (1979) 1079-1112.

[18] B.C. Garrett, D.G. Truhlar, J. Phys. Chem. 83 (1979) 3058.

[19] B.C. Garrett, D.G. Truhlar, J. Phys. Chem. 87 (1983) 4553.

[20] B.C. Garrett, D.G. Truhlar, J. Am. Chem. Soc. 101 (1979) 4534-4548.

[21] C. Eckart, Phys. Rev. 35 (1930) 1303-1309.

[22] H. Johnston, Gas Phase Reaction Rate Theory, New York, Ronald, 1966.

[23] J. Espinosa-García, F.J. Olivares del Valle, J.C. Corchado, Chem. Phys. 183 (1994) 95-100.

[24] J.R. Barker, N.F. Ortiz, J.M. Preses, L.L. Lohr, A. Maranzana, P.J. Stimac, T.L. Nguyen, T.J.D. Kumar, MultiWell-2014.1 Software, University of Michigan, Ann Arbor, Michigan, 2014, http://aoss.engin.umich.edu/multiwell/.

[25] M.A. Harthcock, J. Laane, J. Phys. Chem. 89 (1985) 4231-4240.

[26] L. Chen, K. Tokuhashi, S. Kutsuna, A. Sekia, Int. J. Chem. Kinet. 36 (2004) 26-33.

[27] M.J. Kurylo, V.L. Orkin, Chem. Rev. 103 (2003) 5049-5076.

[28] R.G. Prinn, J. Huang, R.F. Weiss, D.M. Cunnold, P.J. Fraser, P.G. Simmonds, A. McCulloch, C. Harth, P. Salameh, S. O'Doherty, R.H.J. Wang, L. Porter, B.R. Miller, Science 292 (2001) 1882-1888.

[29] J. Zheng, D.G. Truhlar, Phys. Chem. Chem. Phys. 12 (2010) 7782-7793.

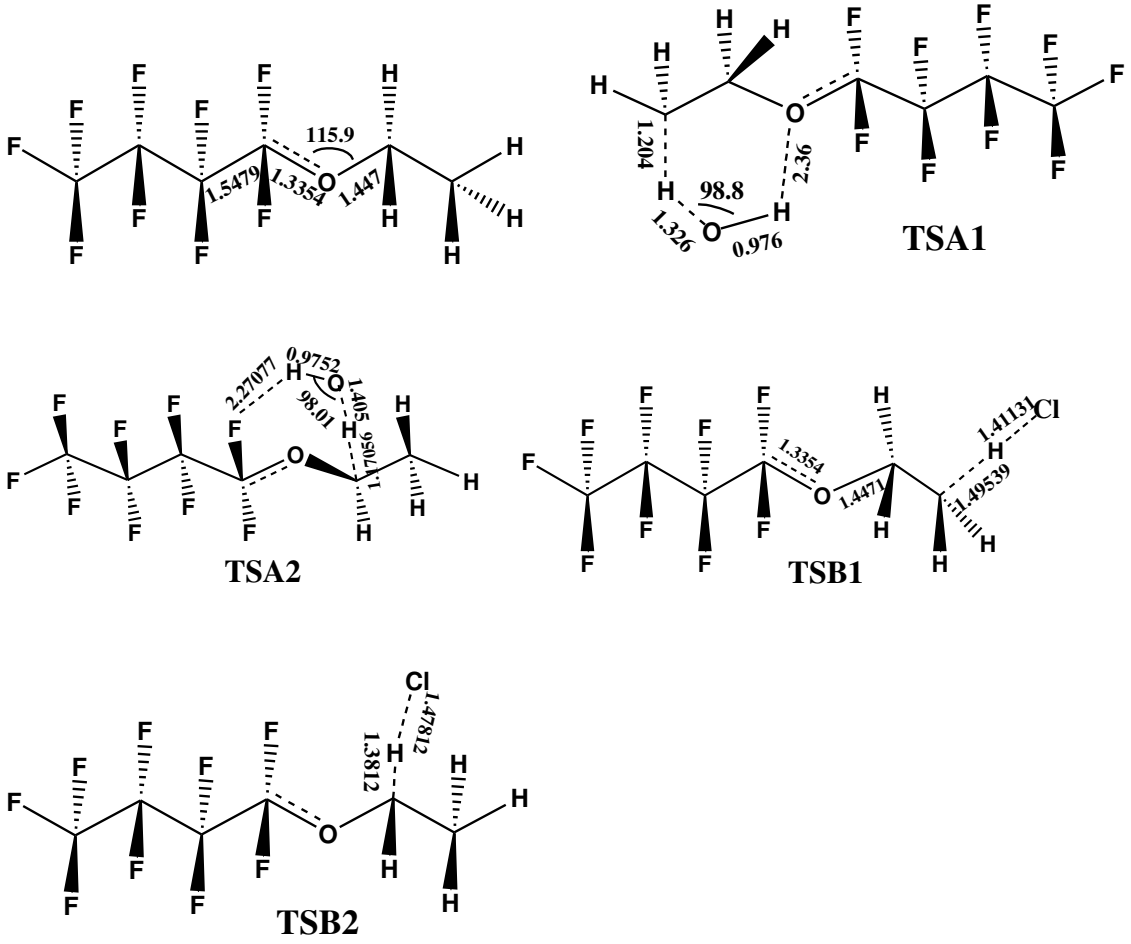

Figure 1. The geometries of reactant and the transition states arising from the reaction of $C_4F_9OC_2H_5$ with OH and Cl radicals (the z-matrices are given as Supplemental Information).

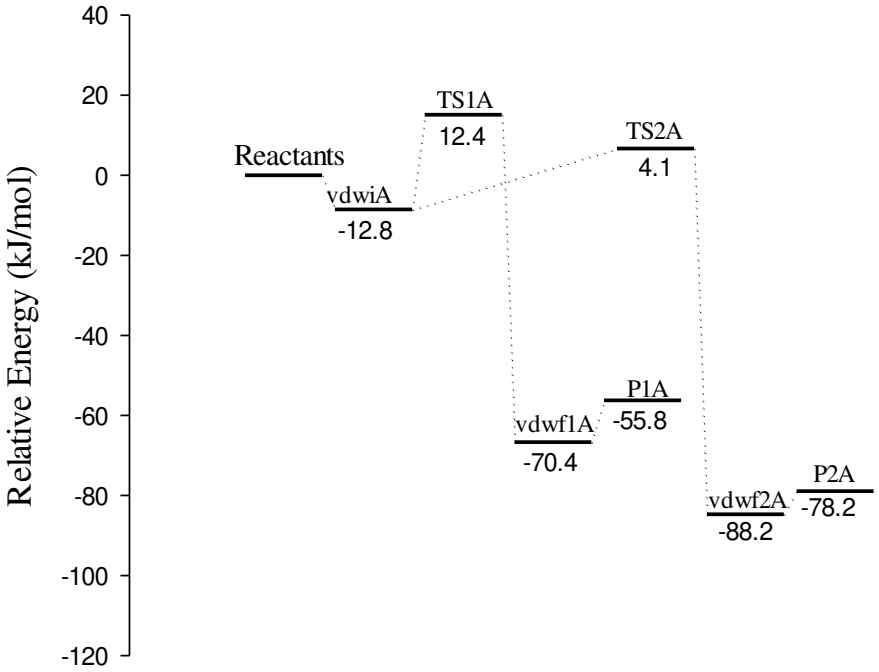

Figure 2. Relative energies of the stationary points located on the doublet ground-state potential energy surface of the $C_4F_9OC_2H_5$ + OH reaction, calculated at the MPWB1K/MG3S level of theory.

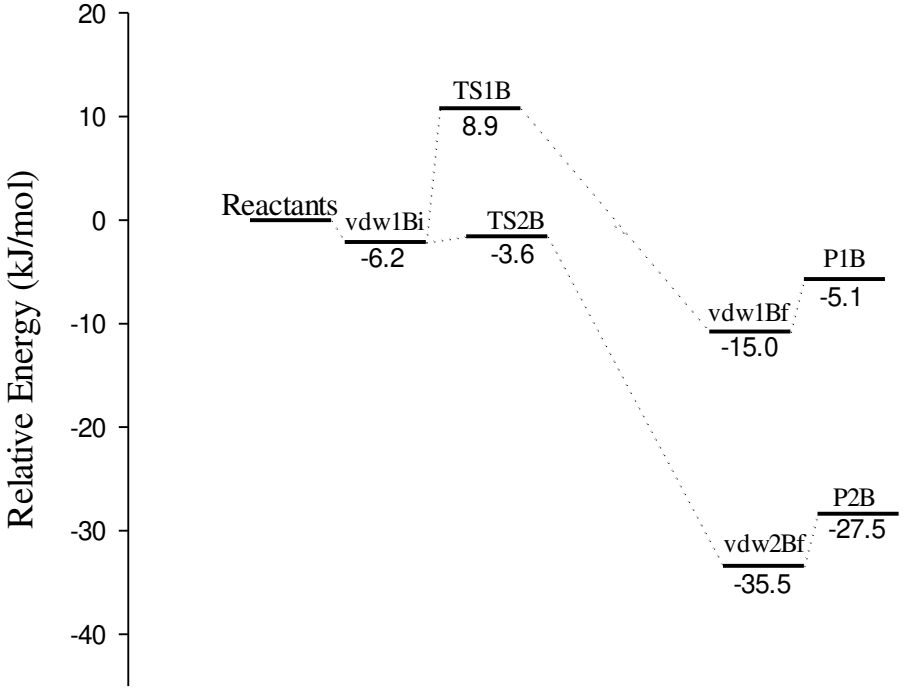

Figure 3. Relative energies of the stationary points located on the doublet ground-state potential energy surface of the $C_4F_9OC_2H_5$ + Cl reaction, calculated at the MPWB1K/MG3S level of theory.

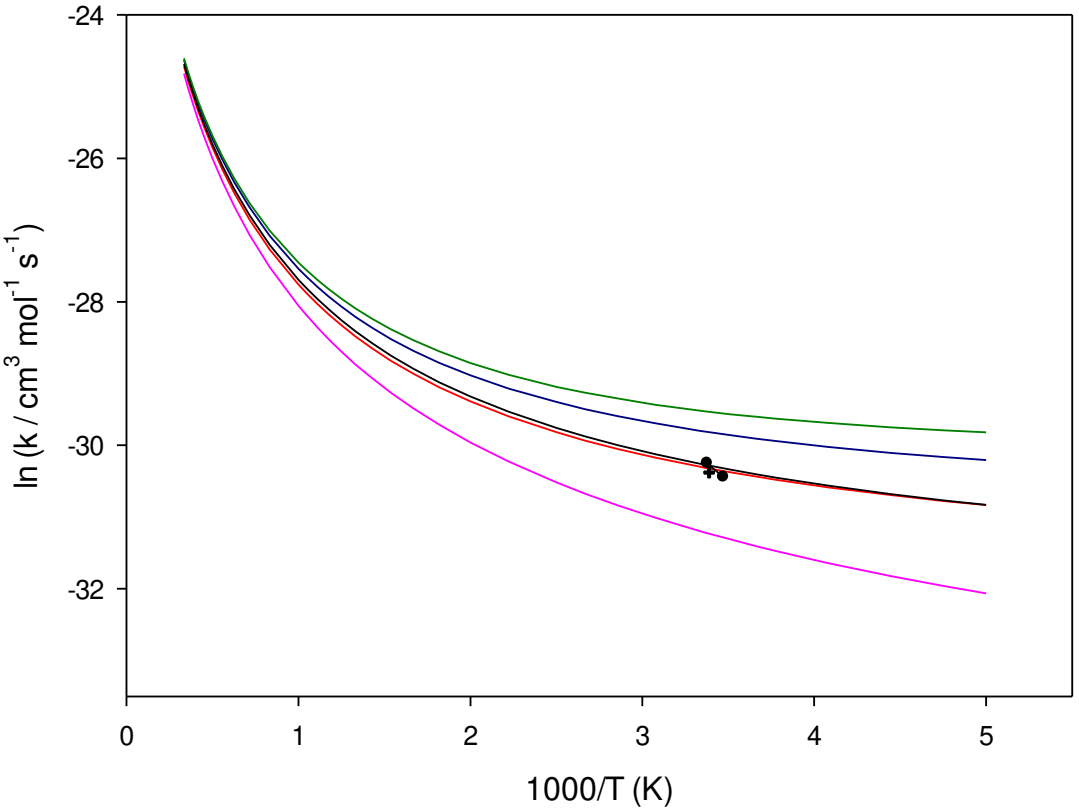

Figure 4. The thermal rate coefficients for the $C_4F_9OC_2H_5$ + OH reaction computed at temperatures in the range of 200-2000 K. The pink, blue, red, green, black lines are computed by using BB1K/MG3S, KMLYP/6-311++G(2d,2p), MPWB1K/MG3S, M06-2X/MG3S and M05-2X/MG3S respectively. Experimental data are given for the purpose of comparison. (+) from Ref. 2, (●) from Ref. 3.

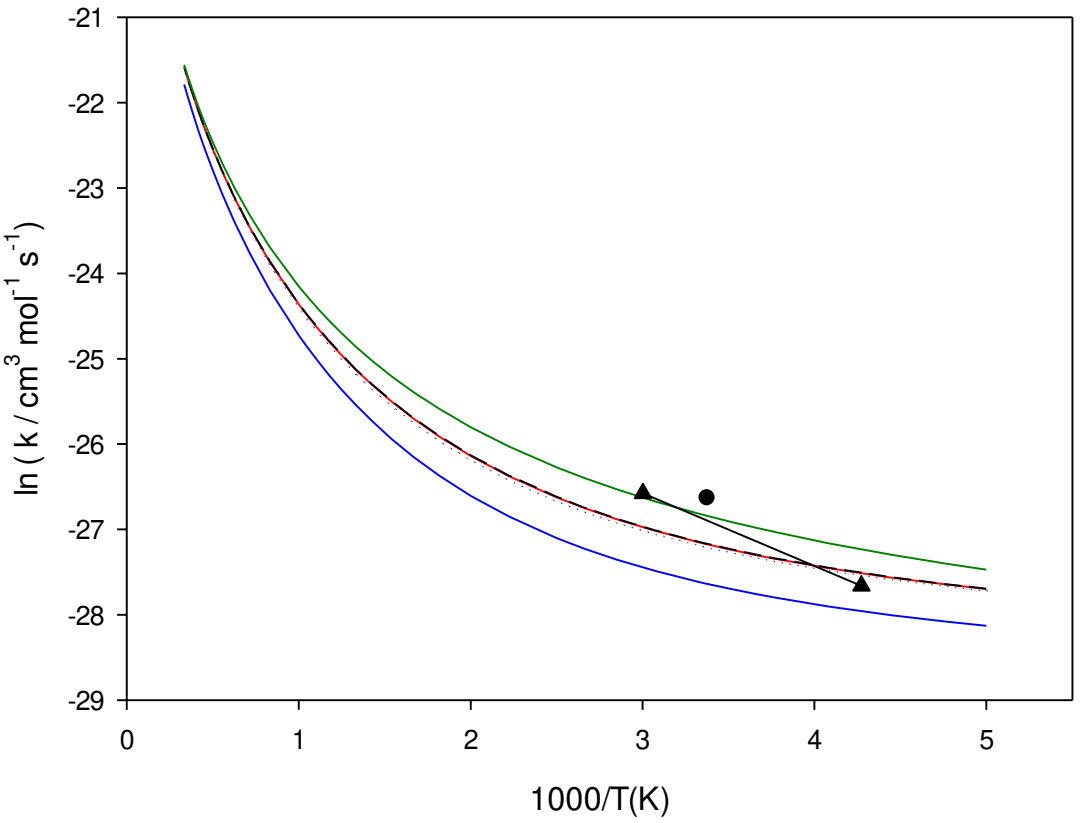

Figure 5. The thermal rate coefficients for the $C_4F_9OC_2H_5$ + Cl reaction computed at temperatures in the range of 200-2000 K. The blue, red, green, black dotted and black dashed lines are computed by using BB1K/MG3S, KMLYP/6-311++G(2d,2p), M05-2X/MG3S, MPWB1K/MG3S and M06-2X/MG3S respectively. Experimental data are given for the purpose of comparison. (●) from Ref. 2, (▲) from Ref. 4.

Table 1. The energies of the stationary points relative to their reactants for the reactions

	BB1K	M052X	M062X	MPWB1K	KMLYP
VwdiA	-8.5	-19.3	-14.4	-12.8	-16.5
TS1	15.1	8.0	7.2	12.4	14.5
Vdw1Af	-66.7	-86.3	-88.2	-70.4	-75.9
P1A	-56.3	-64.5	-63.8	-55.8	-57.7
TS2A	6.7	4.6	1.5	4.1	5.8
Vdw2Af	-84.7	-97.7	-101.5	-88.2	-88.9
P2A	-78.9	-82.3	-82.9	-78.2	-76.5
Vwd1Bi	-2.1	-13.4	-16.7	-6.2	-9.7
TS1B	10.8	3.3	8.0	8.9	8.2
Vdw1Bf	-10.8	-20.2	-23.5	-15.0	-31.8
P1B	-5.7	-3.7	-3.8	-5.1	-1.4
TS2B	-1.6	-3.7	-4.2	-3.6	0.0
Vdw2Bf	-33.4	-35.4	-37.0	-35.5	-33.0
P2B	-28.4	-21.4	-23.0	-27.5	-20.3

R_A and R_B computed by different DFT methods in kJ mol^{-1}.